Valence photoionization and the following fragmentation pathways in Sb_4 clusters

S. Urpelainen,[1,*] A. Caló,[1] L. Partanen,[1] M. Huttula,[1] J. Niskanen,[1,2] E. Kukk,[3] S. Aksela,[1] and H. Aksela[1]
[1]*Department of Physics, University of Oulu, P.O. Box 3000, Oulu 90014, Finland*
[2]*Theoretical Chemistry, Royal Institute of Technology, Roslagstullsbacken 15, S-106 91 Stockholm, Sweden*
[3]*Department of Physics and Astronomy, University of Turku, FIN-20014 Turku, Finland*
(Received 8 June 2009; published 1 October 2009)

The valence photoelectron spectrum of Sb_4 clusters and the following fragmentation patterns have been studied using synchrotron radiation and electron-ion coincidence technique. An experimental photoelectron spectrum of the $5t_2$ ionization of Sb_4 is presented. Theoretical molecular calculations, together with the existing data on the noble gas xenon, were used to describe the experimental results. The bonding properties of the molecular orbitals involved are used to qualitatively describe the dissociation process.

DOI: 10.1103/PhysRevA.80.043201 PACS number(s): 36.40.Qv, 36.20.Kd, 32.80.Fb

I. INTRODUCTION

Clusters are particles formed from only a few to up to thousands of bound atoms or molecules. Clusters represent an ideal link that allows connecting smoothly the properties of single atoms and molecules to the properties of solids, providing an excellent opportunity to study the gradual development of collective properties that characterize a bulk solid (i.e., electric conductivity, magnetic properties, etc.). In this sense small metal clusters in particular provide an excellent target as their physical properties are highly size dependent. In this framework antimony (Sb) clusters are a very interesting subject. Sb and its compounds are commonly used elements in manufacturing semiconductor devices and in many other industrial processes. Furthermore, the production of small Sb clusters is relatively simple and there is no need for a specialized cluster source as Sb evaporates readily as small—predominantly Sb_4—clusters at relatively low temperatures [1]. Nevertheless, no extensive studies of the electronic structure of Sb_4 cluster have been carried out. Most of the studies dated back to the 1980s and 1990s, when the valence shell of Sb, Sb_2, Sb_4, and Sb_8 clusters have been studied using HeI photoelectron spectroscopy [2–7]. More recently Urpelainen *et al.* performed a study on the $4d$ photoionization, subsequent Auger decay, and fragmentation pathways of Sb_4 clusters [8].

The electronic configuration of an antimony atom in its ground state is $[Kr]4d^{10}5s^25p^3$. In the molecular orbital (MO) picture and the T_d point group, the valence electronic configuration of Sb_4 clusters is

$$(4a_1)^2(5t_2)^6(5a_1)^2(6t_2)^6(2e)^4,$$

with the $^1A_1$ ground state. The three outermost MOs $5a_1$, $6t_2$, and $2e$ are mainly linear combinations of the atomic Sb $5p$ orbitals and present a nonbonding character, except for the $2e$ MO, which is an Sb-Sb bonding orbital. The $5t_2$ and the $4a_1$ MOs are mainly linear combination of atomic Sb $5s$-like orbitals and present bonding character. The lowest unoccupied molecular orbital (LUMO) is composed mainly of Sb $5p$ orbitals and has a clear antibonding character [4,8]. As its nearest atomic closed-shell counterpart, the noble gas xenon atom can be used as a comparison for the electronic transitions involving MOs consisting of atomic $5s$ orbitals in the Sb_4 cluster.

In this work we present an experimental study of the Sb valence photoionization and the following fragmentation patterns using the photoelectron-photoion coincidence (PEPICO) technique, which has proven to be an excellent tool for fragmentation studies [9–13]. Experimental results have been compared with theoretical molecular calculations and with the existing data on the noble gas xenon.

II. EXPERIMENTS

The experiments were performed on the high-resolution soft x-ray undulator beamline I411 on the 1.5 GeV MAX II storage ring in MAX-laboratory (Lund, Sweden) [14]. The experimental setups were mounted on the so-called 1 m section of the beamline. The valence photoelectron spectrum was recorded using a modified Scienta SES-100 electron energy analyzer mounted on the experimental station built in Oulu [15,16]. The PEPICO events were recorded using an electron-ion coincidence apparatus consisting of the same SES-100 hemispherical electron energy analyzer and a Wiley-McLaren-type ion time-of-flight (TOF) spectrometer built in Turku. A detailed description of the apparatus can be found in Ref. [17]. The measurements were carried out at the magic angle of 54.7° with respect to the electric field vector of the incoming radiation.

When measuring the photoelectron spectrum, an inductively heated oven equipped with a single holed Mo crucible built in Oulu [18] was used to produce the Sb_4 cluster beam at temperatures around roughly 1300 °C. The use of such high temperatures allowed the rapid decrease in the amount of common residual gases (such as H_2O, CO_2, etc.) and a high vapor pressure, and thus a very pure signal of antimony in the valence photoelectron spectrum. The background pressure of the chamber during the experiments was in the 10^{-7} mbar range.

For producing the cluster beam in the coincidence measurements, a commercial resistively heated oven (MBE Komponenten, model NTEZ-40) with an open pyrolytical boron nitride crucible was used. The temperature of the oven dur-

*samuli.urpelainen@oulu.fi

ing the measurements was around 470 °C corresponding to vapor pressure on the order of approximately 10^{-3} mbar within the heated volume [19]. The background pressure was on the order of 10^{-7} mbar.

The valence photoelectron spectrum and the PEPICO events were recorded using photon energies of 60 and 60.5 eV, respectively. The photoelectron spectrum was recorded using a constant spectrometer pass energy of 20 eV. The monochromator exit slit and the electron energy analyzer entrance slit were chosen to be 100 μm and 0.8 mm (curved), respectively. These values correspond to a photon bandwidth of 40 meV and an analyzer broadening of approximately 80 meV. For recording the PEPICO events, the pass energy of the electron analyzer was set to 100 eV, corresponding to an analyzer energy window width of approximately 11 eV. The electron energy analyzer entrance slit was 1.6 mm. The extraction pulse voltages of the ion TOF spectrometer during the measurements were +200 and −221 V and the pulse duration was 30 μs. The acceleration voltage was 1190 V. The monochromator exit slit was closed to a minimum in order to maintain a good purity of the coincidence signal (see Ref. [17] and references therein).

III. RESULTS AND DISCUSSION

At the experimental conditions described in Sec. II, the evaporation from bulk Sb shows a predominant production of Sb_4 clusters in which the atoms are likely to be packed in tetrahedral geometry [1]. According to Dyke *et al.* [7], temperatures in the range of 1400 °C are needed with a superheated oven configuration in order to break the Sb_4 clusters to smaller species. The production of smaller Sb_3, Sb_2, and Sb was monitored in the superheating conditions by measuring the valence photoelectron spectrum and the 4*d* photoelectron spectrum. Neither of these showed any significant changes at the temperatures used in the experiments and thus no peaks arising from smaller species are expected to show in the spectra. During the coincidence measurements, ion TOF mass spectra were recorded to see if larger clusters are present in the sample region. No such species were observed. These two observations and the existing literature led us to conclude that the vapor consists mainly of Sb_4 clusters and clusters of other sizes have negligible contribution.

Theoretical calculations for molecular single vacancy energy states were performed using GAMESS software package [20,21]. The electronic structure and the ionization energies were determined using occupation restricted multiple active space (ORMAS) [22,23] determinant configuration-interaction (CI) calculation with a large orbital-small core potential [CRENBL effective core potential (ECP)] basis set [24]. Also a complete active space (CAS) -CI calculation with a virtual space of three orbitals using the GAMESS package was performed in order to study singly ionized excited states. Active orbitals in the CAS-CI calculation were $4a_1$, $5t_2$, $5a_1$, $6t_2$, and $2e$ and all orbitals were optimized for the lowest $2e^{-1}$ ionized state. These calculations were performed using augmented correlation-consistent polarized valence-double-zeta (aug-cc-pVDZ) basis set with effective core potentials [25,26].

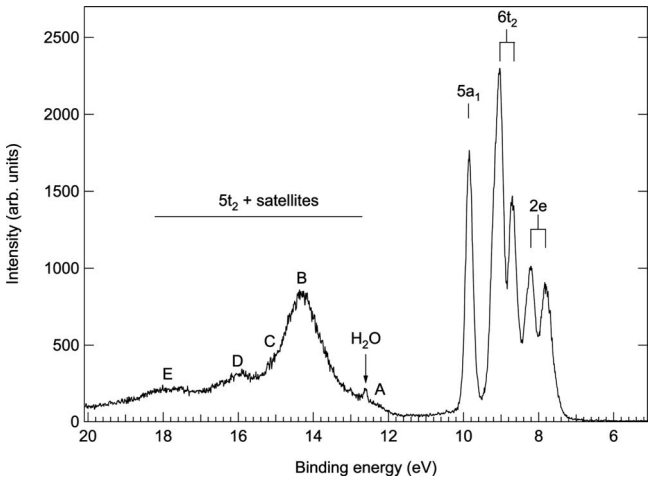

FIG. 1. Valence photoelectron spectrum of Sb_4 with assignment. MOs are assigned according to the T_d geometry.

The experimental and the computational results from the ORMAS calculations are summarized in Fig. 1 and Table I. The five intense bands between 7 and 11 eV are well known from previous works [2,3,7] and they are produced by the photoionization of the three outer MOs. The ionization creates $^2E(2e^{-1})$, $^2T_2(6t_2^{-1})$, and $^2A_1(5a_1^{-1})$ states. The first two states are degenerate and Jahn-Teller active as the tetrahedral geometry of the ions is unstable in these states against asymmetric vibration. The splitting of these states in the photoelectron spectrum (PES) is determined by the combined effect of the Jahn-Teller and the spin-orbit interactions [3].

In a previous study [2], additional features between 10.5 and 16 eV were observed but were too weak to be carefully analyzed and were tentatively assigned to antimony 5*s*-like MOs and shake-up lines. In the spectra recorded in this work these features are much stronger, and despite the overlap with the weak signal from the common residual gases (H_2O, CO, CO_2, etc.) a multiple band structure is clearly visible

TABLE I. Binding energies of the Sb_4 valence orbitals.

	Calc.[a]	Expt.[b]	Expt.[c]	Expt.[d]
$2e$	7.62	7.78	7.81	7.84
		8.20	8.22	8.20
$6t_2$	8.61	8.69	8.70	8.69
		9.01	9.06	9.06
		9.18		
$5a_1$	9.81	9.82	9.74	9.82
$5t_2$	16.72	12.58 (A)		
		14.32 (B)		
		15.16 (C)		
		15.96 (D)		
		17.71 (E)		
$4a_1$	22.52			

[a]ORMAS.
[b]This work.
[c]From Ref. [7].
[d]From Ref. [2].

between 11 and 20 eV. This can be explained by the fact that the previous studies were performed using HeI radiation (21.22 eV), while in the present study a photon energy of 60.5 eV was used. This energy is located on the rising edge of the Sb_4 $4d \rightarrow \epsilon f$ shape resonance [27], which enhances the photoionization cross section of the $4d$ electrons as well as the valence electrons. Similar enhancement of the $5s$ and $5p$ electron photoionization cross section due to the $4d$ giant resonance in Xe has been observed earlier by Becker *et al.* [28]; in Ba, La, and Ce by Richter *et al.* [29]; and in I by Nahon *et al.* [30]. As mentioned earlier, Xe can be used as the reference for the electronic transitions in the Sb_4 cluster and the Sb_4 $5t_2$ MO can be described as a linear combination of Sb $5s$-like atomic orbitals. This suggests that Sb $5s$-like MOs in Sb_4 clusters present a similar behavior on the shape resonance as the $5s$ orbitals in atomic Xe. In a study performed by Dyke *et al.* [7] (and references therein) the lack of lines in this energy region is also attributed to a very low photoionization cross-section ratio between $5s$ and $5p$ in atomic antimony. We expect the much higher intensity of the lines at the 60.5 eV photon energy to be a consequence of these two effects.

Looking at the electron spectrum alone, five separate bands (A–E in Fig. 1) can be distinguished. A comparison to previous work on P_4 clusters that present the same tetrahedral geometry and similar electronic structure as the Sb_4 clusters by Brundle *et al.* [31] is also made. Brundle *et al.* attributed the splitting of the $5t_2^{-1}$ state of P_4 into three components to a strong Jahn-Teller interaction. This however is not believed to be the whole truth in light of the present experimental evidence on Sb_4 and we also consider the argument discussed, but dismissed by Brundle *et al.*, that would assign the several bands observed to various overlapping lines arising from a simultaneous ionization and excitation (shake-up) of valence electrons with a final state of $(5a_1 6t_2 2e)^{-2} nl'$ or a configuration interaction between the $5t_2^{-1}$ and the $(5a_1 6t_2 2e)^{-2} nl$ states, which lie close in energy.

In the first approximation the binding energies for the $(5a_1 6t_2 2e)^{-2} nl'/nl$ states are the sum of the binding energy of the ionized MO and the excitation energy of the second electron. From experimental photoion yields [32] and an experimental electron energy loss spectrum [33], we can state that the excitation energies for the Rydberg-like excitations starts from approximately 3.6 eV and continue up to the ionization threshold of the $5a_1$ orbital. Thus, the binding energy range of simultaneous ionization and excitation becomes approximately 11.4–19.7 eV. The experimental evidence supports this conclusion as the observed bands are spread in the range of 11–20 eV. According to the ORMAS calculations, the binding energy of the $5t_2^{-1}$ state is 16.72 eV (Table I), resulting in a near degeneracy with the $(5a_1 6t_2 2e)^{-2} nl$ states and a breakdown of the one-electron picture. This behavior is seen in the periodic table time to time to smear out the single peak structure (see, e.g., Refs. [34–40] and references therein). For instance, in the noble gas Xe the $5s$ photoline is replaced with a rich structure often referred to as configuration-interaction satellites [35]. We will from now on refer to the correlated $c_1|5t_2^{-1}\rangle + c_2|(5a_1 6t_2 2e)^{-2} nl\rangle$ states together as "$5t_2^{-1}$" states as the intensity of a $5t_2^{-1}$ line is distributed to a many-fold of lines due to heavy mixing of single configuration states. Such a behavior has been observed earlier, for example, in the valence photoionization of CF_4, where corresponding structures have been assigned as correlation satellites occurring due to the breakdown of orbital picture of ionization [41].

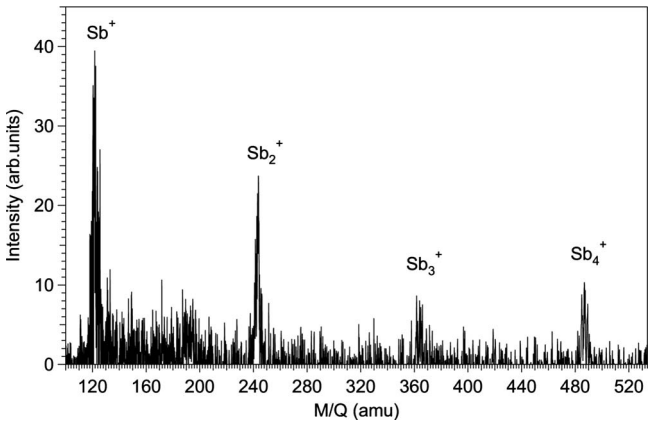

FIG. 2. A TOF mass spectrum converted to mass-to-charge scale recorded in coincidence with the photoelectrons presented in Fig. 1.

It would be tempting to follow the reasoning of Brundle and co-workers and assign three of the bands in the range of 11–20 eV in Fig. 1 to the pure $5t_2^{-1}$ state with a strong Jahn-Teller splitting without paying any attention to the correlation. Keeping the failure of the one-electron picture in mind, however, the bands labeled from A to E may also be assigned to an ionization from "$5t_2$" MOs.

On the other hand A could be assigned to a band arising from an ionization accompanied by a shake-up transition from the three outermost MOs corresponding to $(5a_1 6t_2 2e)^{-2} nl'$ final states. Similar shake-up transitions have been observed earlier in the $4d$ photoelectron spectrum of Sb_4 clusters [8]. The shake-up of the outermost electron due to a rapid relaxation of the charge distribution transfers approximately 10% of the intensity of the main lines to the satellites [35,42]. Band A however is only the first transition in the series of shake-up satellites that continue up to the direct double ionization threshold as in the case of $4d$ ionization and, following this reasoning, bands C–E could be also thought to be a part of this shake-up satellite structure.

Assigning these heavily overlapping and broad spectral bands from the electron spectrum alone is not unambiguous or feasible and thus the PEPICO technique has been employed to study the fragmentation of the Sb_4 cluster following the valence photoionization. The ionization from MOs with different bonding properties and excitations to strongly antibonding LUMO or Rydberg-like states is expected to produce different kinds of dissociation products, which in turn helps in the interpretation of the electron spectrum.

A TOF mass spectrum recorded in coincidence with the valence photoelectrons is presented in Fig. 2. It can be seen that the most abundant fragment is the Sb^+, followed by a significant contribution of Sb_2^+. The larger fragments Sb_3^+ and Sb_4^+ are less abundant, but clearly observable. No doubly charged fragments are observed, signifying that no second step processes take place after the photoionization of the valence electrons. The relative intensities of the detected frag-

TABLE II. Relative intensities of different ionic species observed in coincidence with valence photoelectrons from the TOF spectrum.

	Sb^+	Sb_2^+	Sb_3^+	Sb_4^+	All ions
All electrons	45	23	12	20	100

ments are presented in Table II. The values were obtained by numerical integration of the TOF spectrum.

The measured PEPICO data are illustrated in Fig. 3 as a two-dimensional (2D) map, and in Fig. 4 a coincidence yield for different ions extracted from Fig. 3 is presented. The 2D map of Fig. 3 has been smoothed several times and removed of negative values occurring due to the nature of data treatment [13] for a better visualization. This causes the seemingly good signal-to-noise ratio of the coincidence yields in Fig. 4 as well as the small artifacts not appearing in the photoelectron spectrum. Thus, attention is not paid to the shape of the features as this could be affected by the data treatment process, but only to the position of the features. In addition the relative intensities of the peak groups extracted from the PEPICO data differ from the relative intensities of the electron spectrum. This is caused by the fact that the detection efficiency of the electron detector is not constant throughout the measured window. It should be also noted that due to the poorer energy resolution of the PEPICO measurement the binding energy scale calibration is not as accurate as for the high-resolution photoelectron spectrum. This combined with the data treatment process described above could cause some minor discrepancies between the spectral features as well as absolute energy values when compared to the high-resolution photoelectron spectrum.

The experimental results shown in Fig. 3 clearly indicate that the ionization of the outermost valence MOs ($5a_1$, $6t_2$, and $2e$) results mainly in the production of Sb_4^+ ions without any further fragmentation with only a small amount of Sb^+ ions present. This is not surprising since in the case of Sb_4 clusters the three outermost valence orbitals are very weakly bonding and nonbonding in nature and thus the removal of

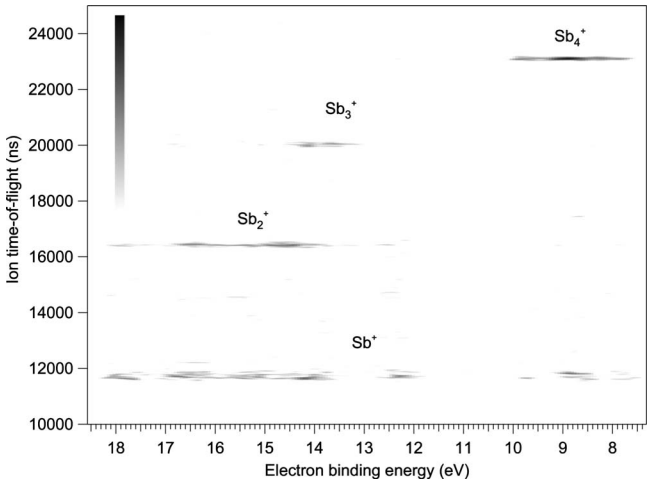

FIG. 3. 2D PEPICO map of the valence photoionization in the TOF region of the observed antimony ions.

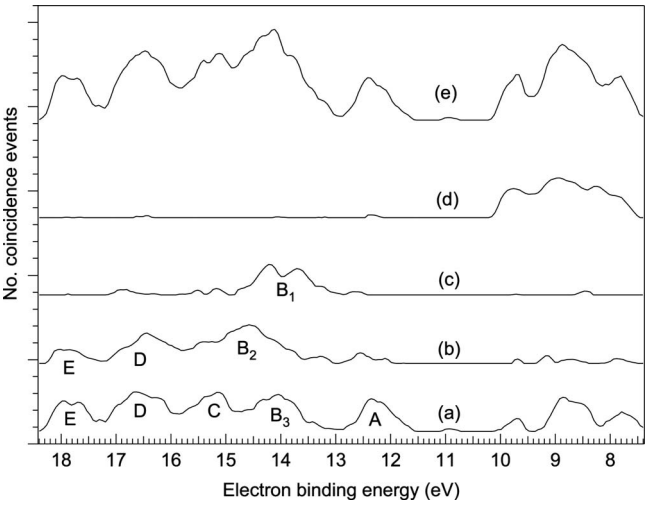

FIG. 4. Extracted coincidence yields from different ions from Fig. 3. Curves (a), (b), (c), (d), and (e) represent coincidence yields extracted from Sb^+, Sb_2^+, Sb_3^+, Sb_4^+, and a sum of all four, respectively. All yields have the same intensity scale.

an electron from these orbitals does not affect the stability of the cluster. The Jahn-Teller active $6t_2^{-1}$ and $2e^{-1}$ states however seem to produce also a considerable amount of Sb^+ fragments. On closer inspection the signal of Sb^+ ions is split into two parts. This is caused by the two naturally occurring isotopes ^{121}Sb and ^{123}Sb with natural abundances of 57.2% and 42.8%, respectively. This splitting was already observed earlier in the case of $4d$ photoionization and the following fragmentation [8]. All in all Fig. 3 shows that most of the fragmentation takes place only after ionization from the inner valence $5t_2^{-1}$ states and in fact no significant amount of Sb_4^+ ions is observed in coincidence with these electrons.

Looking at Figs. 3 and 4 it can be also clearly seen that band B is in fact composed of three separate bands (B_1, B_2, and B_3), separated significantly in energy, which cannot be resolved in the electron spectrum alone. The difference in fragmentation of these three subbands leads us to suppose that each subband may correspond to a different geometry or Jahn-Teller active state. The production of Sb_3^+ ions is associated only with a small portion of the spectrum, namely, the $5t_2^{-1}$ states (band B in Fig. 1 and band B_1 in Fig. 4). The Sb_2^+ ions are produced together with the three bands B (B_2), D, and E. As band B_2 is clearly shifted toward higher binding energies from band B_1, but not enough to correspond to a shake-up transition, we are lead to believe that it is a Jahn-Teller split component of the $5t_2^{-1}$ state. Bands D and E are also assigned to the correlated $5t_2^{-1}$ states due to a similar fragmentation behavior with band B_2.

The Sb^+ ions are produced together with bands A, B (B_3), and C–E. As band A is assigned to an ionization accompanied by a shake-up transition corresponding to $(5a_1 6t_2 2e)^{-2} nl'$ final states, structures C–E may also contain final states of shake-up character. Band B_3 could be assigned to be another Jahn-Teller split component of $5t_2^{-1}$ final states, but the present experiment does not allow us to conclude whether the intensity of this state is also distributed to bands C–E.

The results of the CAS-CI calculation suggest that structure A in Fig. 4 is formed of ionized states with negligible (less than 0.0025) contributions from $4a_1^{-1}$ and $5t_2^{-1}$ configurations and significant contribution from configurations with holes in the $5a_1$, $6t_2$, and $2e$ orbitals. These calculated states extend 6.19 eV above the $2e^{-1}$ state. This strongly supports the earlier conclusion that structure A is first in a series of shake-up transitions accompanying the $(5a_1 6t_2 2e)$ ionization. Further theoretical assignment of higher excited states within this study was not possible due to the fact that the computational resources needed to perform these heavy calculations were, unfortunately, not available to us at the time.

The dissociation patterns of the $(5a_1 6t_2 2e)^{-2} nl'$ and $5t_2^{-1}$ states can be compared to the dissociation patterns of the $(5a_1 6t_2 2e)^{-2}$ and $(4a_1 5t_2)^{-1}(5a_1 6t_2 2e)^{-1}$ states observed following the N-valence-valence (NVV) Auger decay recorded in Ref. [8]. Although the charge of the cluster is different, the excited shake-up and correlation satellite states have two holes in the orbitals involved in the net bonding of the molecule as one electron is excited to a higher-lying orbital being either an antibonding one or a Rydberg orbital. The results obtained using ion-ion coincidence techniques in Ref. [8] show that the cluster is always dissociating when two valence electrons are removed, and furthermore that in the $(4a_1 5t_2)^{-2}$ region the cluster is mainly fragmented to Sb and Sb_2. Thus, the two holes on the bonding orbitals seem to cause a more complex fragmentation than merely a loss of a neutral atom. Similar behavior has been observed experimentally in BF_3 molecule, where the dissociation following the normal Auger decay, with the two final-state holes on the valence shells, shows no significant differences from the dissociation following the resonant Auger decay with two final-state holes on the valence shells and one electron on a higher-lying MO [43]. It is also observed earlier in small molecules such as CD_4 [44] that the ionization of inner valence electrons tends to be more dissociative and resulting in smaller ionized fragments than that of the outer valence. This behavior is significantly different from larger clusters such as C_{60}, where the dissociation tends to take place as loss of small neutral fragments [45]. The difference in favored fragments could be explained by the fact that in large clusters such as C_{60} the valence bands are highly delocalized (see, e.g., Ref. [46]), whereas small clusters show more molecularlike behavior and the charge in the ionic state is more localized.

IV. CONCLUSIONS

In this work we have presented an assignment for the Sb_4 inner valence photoelectron spectrum with its satellite transitions. Previous discussions for the similar P_4 cluster were used as a comparison and it was found out that the conclusions made by Brundle *et al.* [31] do not seem to apply for Sb_4 clusters as such. Instead, the several additional and overlapping broadbands have been attributed to correlated $5t_2^{-1}$ states and shake-up satellites accompanying the $(5a_1 6t_2 2e)^{-1}$ ionization. Unfortunately these states overlap so heavily in energy that distinguishing between the two different sources of the lines is not possible from the experiments performed in this study. The assignment could be further verified and specified experimentally by studying the electron spectrum, PEPICO, and partial ion yields at the $4d \rightarrow nl$ resonances that decay to the same $(5a_1 6t_2 2e)^{-2} nl$ final states via the resonant Auger process. This experiment is planned to be performed in the near future. In addition angular distribution of the photoelectrons could be recorded and, if they differ significantly for the two different sources of satellite lines, this could be of further help in the interpretation of the spectrum.

It is also concluded that the noble gas Xe serves as an excellent reference for understanding the properties of virtually closed-shell Sb_4 clusters together with theoretical molecular calculations providing a useful tool in identifying the transitions observed in the experimental PES of Sb_4. These methods confirmed the previous experimental results and allowed the identification of the broadband structures as the inner valence $5t_2$ MO distributed to a many-fold of states due to correlation.

The ion TOF and the PEPICO technique serve as very useful tools in further assigning the electron spectra, when the bonding properties of the orbitals taking part in the transitions are known. This would be nearly impossible with the electron spectrum alone as the present computational models are unable to predict the excited states of ionized molecules correctly. The PEPICO method allowed us to study also the fragmentation of the Sb_4 clusters and the experimental results are well in line with the theoretically modeled bonding properties of the MOs, where the electron vacancies are created, and LUMO to which electrons are excited. In addition it was found out that correlation effects through shake-up transitions and correlation satellites play a significant role not only in electronic dynamics, but also in the fragmentation dynamics of singly ionized Sb_4 clusters.

ACKNOWLEDGMENTS

This work was financially supported by the Research Council for Natural Sciences of the Academy of Finland, the European Community Research Infrastructure Action under the FP6 "Structuring the European Research Area" Program (through the Integrated Infrastructure Initiative "Integrating Activity on Synchrotron and Free Electron Laser Sciences") and the Nordforsk network. S.U., M.H., and A.C. would like to thank the Vilho, Yrjö, and Kalle Väisälä Foundation and S.U. acknowledges the Tauno Tönning Foundation and Magnus Ehrnrooth Foundation for financial support. We thank Dr. Rami Sankari for the preparatory work and Dr. Sari Granroth for help during the experiments. We acknowledge the staff of MAX-laboratory for their assistance during the experiments.

[1] K. Sattler, J. Mühlbach, and E. Recknagel, Phys. Rev. Lett. **45**, 821 (1980).
[2] S. Elbel, J. Kudnig, M. Grodzicki, and H. J. Lempka, Chem. Phys. Lett. **109**, 312 (1984).
[3] L. S. Wang, Y. T. Lee, D. A. Shirely, K. Balasubramanian, and P. Feng, J. Chem. Phys. **93**, 6310 (1990).
[4] L. S. Wang, B. Niu, Y. T. Lee, D. A. Shirley, E. Ghelichkhani, and E. R. Grant, J. Chem. Phys. **93**, 6318 (1990).
[5] L. S. Wang, B. Niu, Y. T. Lee, D. A. Shirley, E. Ghelichkhani, and E. R. Grant, J. Chem. Phys. **93**, 6327 (1990).
[6] V. Kumar, Phys. Rev. B **48**, 8470 (1993).
[7] J. M. Dyke, A. Morris, and J. C. H. Stevens, Chem. Phys. **102**, 29 (1986).
[8] S. Urpelainen, A. Caló, L. Partanen, M. Huttula, S. Aksela, H. Aksela, S. Granroth, and E. Kukk, Phys. Rev. A **79**, 023201 (2009).
[9] E. Rühl, Int. J. Mass. Spectrom. **229**, 117 (2003).
[10] A. F. Lago, A. C. F. Santos, and G. G. B. de Souza, J. Chem. Phys. **120**, 9547 (2004).
[11] A. C. F. Santos, C. A. Lucas, and G. G. B. de Souza, Chem. Phys. **282**, 315 (2002).
[12] M. Simon, M. Lavollée, M. Meyer, and P. Morin, J. Electron Spectrosc. Relat. Phenom. **79**, 401 (1996).
[13] E. Kukk, G. Prümper, R. Sankari, M. Hoshino, C. Makochekanwa, M. Kitajima, H. Tanaka, H. Yoshida, Y. Tamenori, E. Rachlew, and K. Ueda, J. Phys. B **40**, 3677 (2007).
[14] M. Bässler, A. Ausmees, M. Jurvansuu, R. Feifel, J.-O. Forsell, P. de Tarso Fonseca, A. Kivimäki, S. Sundin, and S. L. Sorensen, R. Nyholm, O. Björneholm, S. Aksela, and S. Svensson, Nucl. Instrum. Methods Phys. Res. A **469**, 382 (2001).
[15] M. Huttula, M. Harkoma, E. Nõmmiste, and S. Aksela, Nucl. Instrum. Methods Phys. Res. A **467-468**, 1514 (2001).
[16] M. Huttula, S. Heinäsmäki, H. Aksela, E. Kukk, and S. Aksela, J. Electron Spectrosc. Relat. Phenom. **156-158**, 270 (2007).
[17] E. Kukk, R. Sankari, M. Huttula, A. Sankari, H. Aksela, and S. Aksela, J. Electron Spectrosc. Relat. Phenom. **155**, 141 (2007).
[18] M. Huttula, K. Jänkälä, A. Mäkinen, H. Aksela, and S. Aksela, New J. Phys. **10**, 013009 (2008).
[19] R. E. Honig and D. A. Kramer, RCA Rev. **30**, 285 (1969).
[20] M. W. Schmidt *et al.*, J. Comput. Chem. **14**, 1347 (1993).
[21] M. S. Gordon and M. W. Schmidt, in *Theory and Applications of Computational Chemistry: The First Forty Years*, edited by C. E. Dykstra, G. Frenking, K. S. Kim, and G. E. Scuseria (Elsevier, Amsterdam, 2005).
[22] J. Ivanic, J. Chem. Phys. **119**, 9364 (2003).
[23] J. Ivanic, J. Chem. Phys. **119**, 9377 (2003).
[24] L. A. LaJohn, P. A. Christiansen, R. B. Ross, T. Atashroo, and W. C. Ermler, J. Chem. Phys. **87**, 2812 (1987).
[25] K. A. Peterson, J. Chem. Phys. **119**, 11099 (2003).
[26] B. Metz, H. Stoll, and M. Dolg, J. Chem. Phys. **113**, 2563 (2000).
[27] C. Bréchignac, M. Broyer, Ph. Cahuzac, M. de Frutos, P. Labastie, and J.-Ph. Roux, Phys. Rev. Lett. **67**, 1222 (1991).
[28] U. Becker, D. Szostak, H. G. Kerkhoff, M. Kupsch, B. Langer, R. Wehlitz, A. Yagishita, and T. Hayaishi, Phys. Rev. A **39**, 3902 (1989).
[29] M. Richter, M. Meyer, M. Pahler, T. Prescher, E. v. Raven, B. Sonntag, and H. E. Wetzel, Phys. Rev. A **39**, 5666 (1989).
[30] L. Nahon, A. Svensson, and P. Morin, Phys. Rev. A **43**, 2328 (1991).
[31] C. R. Brundle, N. A. Kuebler, M. B. Robin, and H. Basch, Inorg. Chem. **11**, 20 (1972).
[32] R. K. Yoo, B. Ruscic, and J. Berkowitz, J. Electron Spectrosc. Relat. Phenom. **66**, 39 (1993).
[33] S. Urpelainen Ph.D. thesis, University of Oulu, 2009.
[34] H. Aksela, S. Aksela, and H. Pulkkinen, Phys. Rev. A **30**, 2456 (1984).
[35] S. Alitalo, A. Kivimäki, T. Matila, K. Vaarala, H. Aksela, and S. Aksela, J. Electron Spectrosc. Relat. Phenom. **114-116**, 141 (2001).
[36] H. Smid and J. E. Hansen, J. Phys. B **16**, 3339 (1983).
[37] L. O. Werme, T. Bergmark, and K. Siegbahn, Phys. Scr. **6**, 141 (1972).
[38] H. Aksela, S. Aksela, and H. Pulkkinen, Phys. Rev. A **30**, 865 (1984).
[39] S. Southworth, U. Becker, C. M. Truesdale, P. H. Kobrin, D. W. Lindle, S. Owaki, and D. A. Shirley, Phys. Rev. A **28**, 261 (1983).
[40] S. Urpelainen, S. Heinäsmäki, M.-H. Mikkelä, M. Huttula, S. Osmekhin, H. Aksela, and S. Aksela Phys. Rev. A **80**, 012502 (2009).
[41] D. M. P. Holland *et al.*, Chem. Phys. **308**, 43 (2005).
[42] K. Jänkälä, S. Fritzsche, M. Huttula, J. Schulz, S. Urpelainen, S. Heinäsmäki, S. Aksela, and H. Aksela, J. Phys. B **40**, 3435 (2007).
[43] K. Ueda, H. Chiba, Y. Sato, T. Hayaishi, E. Shigemasa, and A. Yagishita, Phys. Rev. A **46**, R5 (1992).
[44] J. Rius i Riu, E. M. García, J. Á. Ruiz, P. Erman, P. Hatherly, E. Rachlew, and M. Stankiewicz, Phys. Rev. A **68**, 022715 (2003).
[45] K. R. Lykke, Phys. Rev. A **52**, 1354 (1995).
[46] M. Nyberg, Y. Luo, L. Triguero, L. G. M. Pettersson, and H. Ågren, Phys. Rev. B **60**, 7956 (1999).